

Phys. Rev. B 21, (1980), and to be published.

<sup>9</sup>E. L. Evans and J. M. Thomas, *J. Solid State Chem.* 14, 89 (1975).

<sup>10</sup>N. Kambe, M. S. Dresselhaus, G. Dresselhaus,

S. Basu, A. R. McGhie, and J. E. Fischer, *Mater. Sci. Eng.* 40, 1 (1979).

<sup>11</sup>A. D. Novaco and J. P. McTague, *Phys. Rev. Lett.* 38, 1286 (1977).

## Fractal Form of Proteins

H. J. Stapleton, J. P. Allen, C. P. Flynn, D. G. Stinson, and S. R. Kurtz

*Department of Physics and Materials Research Laboratory, University of Illinois at Urbana-Champaign, Urbana, Illinois 61801*

(Received 20 March 1980)

Electron spin relaxation measurements on low-spin  $\text{Fe}^{3+}$  in several proteins show that they occupy a space of fractal dimensionality  $d = 1.65 \pm 0.04$ , in conformity with the dimensionality  $d = \frac{5}{3}$  of a self-avoiding random walk. Analysis of myoglobin x-ray data independently confirms this fractal dimension.

PACS numbers: 87.15.By, 63.50.+x, 76.30.-v

We report the temperature dependence of the electron spin relaxation rate of low-spin  $\text{Fe}^{3+}$  in myoglobin azide ( $\text{MbN}_3$ ) and ferricytochrome *c* (CC). We also reanalyze other relaxation data from two low-spin hemoproteins: cytochrome P-450 from *Pseudomonas putida* (CP 450), originally reported by Herrick and Stapleton<sup>1</sup> (denoted by I), and CC.<sup>2</sup> All systems have been studied as frozen aqueous solutions, but single crystals were used in the earlier CC work.<sup>2</sup> Unlike its high-spin counterpart, low-spin iron has no low-lying excited electronic states. The direct and Raman relaxation rates, which in three-dimensional materials vary with temperature  $T$  as  $AT$  and  $CT^9$ , respectively, are therefore not masked by an Orbach (resonant Raman) process.<sup>3</sup> The temperature dependence of the Raman rate measures the density of states in the vibrational spectrum of the material. All our relaxation data are consistent with a Raman rate of the form  $CT^{6.30 \pm 0.07}$ , with  $C$  a constant. The density  $\rho(\omega)$  of vibrational states therefore varies with frequency as  $\omega^{0.65 \pm 0.04}$ . We deduce that the protein has the form of a fractal<sup>4</sup> of dimensionality  $1.65 \pm 0.04$ . Within the experimental uncertainties this is identical with the fractal dimensionality  $d = \frac{5}{3}$  of the self-avoiding random walk (SAW),<sup>4</sup> to which the protein backbone bears a marked resemblance.

The relaxation rates of  $\text{MbN}_3$  and CC were measured directly at 9.5 GHz between 1.5 and 10 K with use of the pulse saturation and recovery technique, with a superheterodyne receiver and fast microwave diode switches. These measurements were limited to rates under  $10^4 \text{ s}^{-1}$ . The

temperature readout and control were accurate to a few millidegrees Kelvin. More experimental details are given in I. Data of Mailer and Taylor for CC were obtained by measuring the phase lag of the magnetic resonance signal under conditions of adiabatic fast passage.<sup>2</sup> These measurements yielded relaxation rates at temperatures between 11 and 18 K.

The Raman relaxation mechanism is a two-phonon process in which a paramagnetic spin flips; one quantum of vibrational energy at  $\omega_1$  is destroyed and another at  $\omega_2$  created, with  $\hbar(\omega_2 - \omega_1) = g\mu_B H$ . At temperatures for which this mechanism is dominant over the direct (one-phonon) relaxation mechanism one can take  $\omega_1 = \omega_2$  to obtain the temperature dependence of the Raman rate as

$$\frac{1}{T_{1R}} \propto \int_0^{\omega_{\max}} \rho^2(\omega) \omega^4 f(\hbar\omega/kT) d\omega, \quad (1)$$

with  $\rho(\omega)$  the density of vibrational states and  $f(z) = e^z / (e^z - 1)^2$ . The creation of one, and the destruction of another, vibrational quantum introduces two of the four powers of  $\omega$  into Eq. (1). The remaining two powers must be present if the interaction is electrostatic in nature and the ion possesses an odd number of electrons.<sup>3</sup>

If we postulate a power law  $\rho(\omega) \propto \omega^p$  for the density of states, the Raman rate of Eq. (1) must vary with temperature  $T$  as

$$\frac{1}{T_{1R}} \propto \left(\frac{kT}{\hbar}\right)^{5+2p} F_{4+2p}(\Theta/T). \quad (2)$$

Here  $\Theta \equiv \hbar\omega_{\max}/k$  and  $F_{4+2p}(\Theta/T)$  is a function

which is constant for  $T \ll \Theta$  and varies as  $T^{-(3+2p)}$  in the classical two-phonon limit where  $T \gg \Theta$ . In a three-dimensional solid,  $p=2$ . Equation (2) then predicts a  $T^9$  Raman rate at low temperatures and a  $T^2$  rate at high temperatures. This  $T^9$  dependence is well established experimentally<sup>3,5,6</sup> for crystals containing dilute concentrations of paramagnetic ions with an odd number of electrons. Low-spin  $\text{Fe}^{3+}$  in potassium cobaltcyanide exhibits a dependence of this type.<sup>7,8</sup>

The case of hemoproteins is unusual. Herrick and Stapleton<sup>1</sup> point out that the Raman rate up to 13 K follows closely a temperature dependence given by  $T^7 F_6(75/T)$ . This corresponds to a two-dimensional density of states ( $p=1$ ) with a sufficiently low value of  $\Theta$  that  $F_6(75/T)$  drops by 63% between 4.2 and 12.9 K. This reduces the logarithmic derivative of  $T^7 F_6(75/T)$  from 7.0 (the low-temperature limit) to 4.4 at 13 K, and to 3.6 at 17.6 K. The planar structure of the heme group was suggested as the origin of this temperature dependence. It was assumed that  $\Theta$  varied among hemoproteins, and that a higher value than 75 K would be required for CC in order to explain the strict power-law dependence of  $1/T_{1R}$  even at 18.5 K.<sup>9</sup>

Relaxation data for CP450,  $\text{MbN}_3$ , and CC are shown in Fig. 1 with the power laws which best fit the Raman rates. The CC relaxation rates between 11 and 18 K, indicated by crosses and obtained from Ref. 2, have been reduced by a factor of 0.106 to bring them into agreement with our pulse saturation data so that an overall temperature dependence of  $T^{6.34}$  could be measured. The dashed line falling below the crosses in Fig. 1 is a high-temperature extrapolation of the best fit utilizing the two-dimensional model [Eq. (2) with  $p=1$ ] and our CC pulse-saturation data. The corresponding value of  $\Theta$  is  $66.7 \pm 4.1$  K. Similar fits of the  $\text{MbN}_3$  and CP450 data yield  $\Theta = 73.1 \pm 3.1$  K and  $75.0 \pm 1.5$  K, respectively.<sup>10</sup>

Blum and Ohnishi<sup>11</sup> report power saturation studies on ferricytochrome *c* and fit their data between 6 and 25 K to a  $T^{5.5}$  law. Pulse saturation studies on a nonheme, iron-sulfur protein<sup>12</sup> yielded relaxation rates varying with temperature as  $0.9 \times T^2 + 3.5 \times 10^{-10} \times T^9 F_8(60/T)$  between 1.5 and 12 K. This value of  $\Theta = 60$  K should be compared with 57.5 K used in fitting our CP450 data to a  $p=2$  model.<sup>10</sup>

These studies demonstrate that below 15 K relaxation rates can be explained by standard models with  $p$  equal 1 or 2 *only* if one assumes a low  $\Theta$  which varies *only* slightly from protein to pro-

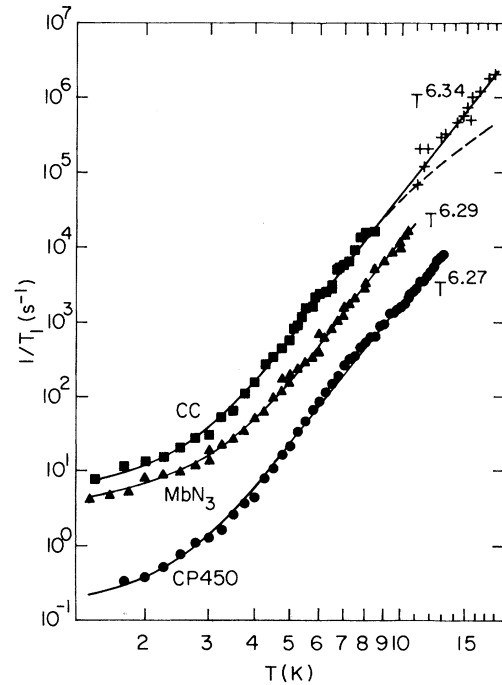


FIG. 1. The electron spin relaxation rate of low-spin  $\text{Fe}^{3+}$  in three hemoproteins, from this work and Refs. 1 and 2. The rates are fitted to the sum of a direct process, varying as  $T$ , and the Raman process corresponding to a fractional dimensionality of approximately  $\frac{5}{3}$ .

tein. However, in those proteins for which measurements have been made to higher temperatures, a simple power-law behavior is maintained, in contradiction to the assumption. This is true for proteins with and without planar substructures.

We infer from these results that the success of the two-dimensional model proposed in I was fortuitous, and that the relaxation rates follow a noninteger-power law. A fit of the Raman data in Fig. 1 to a  $T^n$  power law yields  $n = 6.34 \pm 0.06$ ,  $6.29 \pm 0.08$ , and  $n = 6.27 \pm 0.06$  for the CC,  $\text{MbN}_3$ , and CP450 data, respectively. From Eq. (2) we thus find that all of our pulse-saturation data on relaxation rates in hemoproteins are consistent with a density of vibrational states  $\rho(\omega)$  at the  $\text{Fe}^{3+}$  site which varies with  $\omega$  as the  $0.65 \pm 0.04$  power.

This result can be related in an elegant way to the form of the protein molecule. Suppose that an elastic object consists of  $N$  identical units of mass  $M$ , linked to form a body which is homogeneous and isotropic. Its linear extent  $L$  is given by  $L^d \propto N$ , where  $d$  is, by definition, the fractal dimensionality of the object. For a bulk

deformation which maps the body into its analog of volume  $N(1 - \epsilon)$  the decrease of length is  $\Delta L = L\epsilon/d$ ; the elastic energy is  $Nc\epsilon^2/2$ , with  $c$  the appropriate elastic constant describing each element. The deformation is a straight line along the axis  $\xi$  in the configuration space of the  $N$  units, for which the elastic energy is  $\frac{1}{2}M\omega^2\xi^2$ , with  $\omega$  the vibrational frequency. Changing to cyclic boundary conditions for simplicity, so that each element projects equally on  $\xi$ , we have  $\xi^2 \propto N(\Delta L)^2 \propto NL^2\epsilon^2$ , and hence, from the two expressions for the elastic energy,

$$\omega \propto (c/M)^{1/2}L^{-1} \propto (c/M)^{1/2}N^{-1/d}. \quad (3)$$

The variation of  $\omega$  with  $N$  can be used to deduce the state density by means of the following scaling argument. When  $m$  objects of size  $N/m$  are linked to make  $N$ , the minor change of boundary conditions leaves the density of states unperturbed. Thus  $\rho_N(\omega) = m\rho_{N/m}(\omega)$ , in which the subscripts identify the size. Also, if the normal-mode frequencies vary with  $m$  as  $\omega/m^\alpha$ , we know from scaling that  $\rho_{N/m}(\omega) = m^{-\alpha}\rho_N(\omega/m^\alpha)$ , so that

$$\rho_N(\omega) = m^{-\alpha+1}\rho_N(\omega/m^\alpha). \quad (4)$$

In these expressions the factor  $m^{-\alpha}$  accommodates the reduced energy interval between states. On substituting a density of states  $\rho(\omega) \propto \omega^p$  in Eq. (4), we find  $p = \alpha^{-1} - 1$ . Since, from Eq. (3),  $\alpha = d^{-1}$ , we have  $p = d - 1$  and therefore

$$\rho(\omega) \propto \omega^{d-1}. \quad (5)$$

Equation (5) reproduces the standard power laws  $\omega^0$ ,  $\omega^1$ , and  $\omega^2$  for systems having  $d = 1, 2$ , and  $3$ , respectively. It is more general, however, holding for arbitrary, even fractional,  $d$  as outlined above.

In its application to proteins the generality is important. The exponent  $p = 0.65 \pm 0.04$  in the vibrational spectrum shows that the protein occupies a space of fractal dimensionality  $d = 1.65 \pm 0.04$ . This result is remarkably plausible. The SAW has a theoretical dimensionality<sup>13</sup> of  $\frac{5}{3}$  as verified by numerical methods to about 1%.<sup>14</sup> Its non-self-intersecting character and sinuous backbone lend the protein form a character noticeably similar to the SAW. Our relaxation measurements have evidently probed this form through the way it determines the vibrational spectrum.

The analogy between the protein and the SAW is open to direct experimental verification with use of the x-ray data of myoglobin at 250 K.<sup>15</sup> Figure 2 shows the variation of the number of alpha carbons with distance, as explained in the

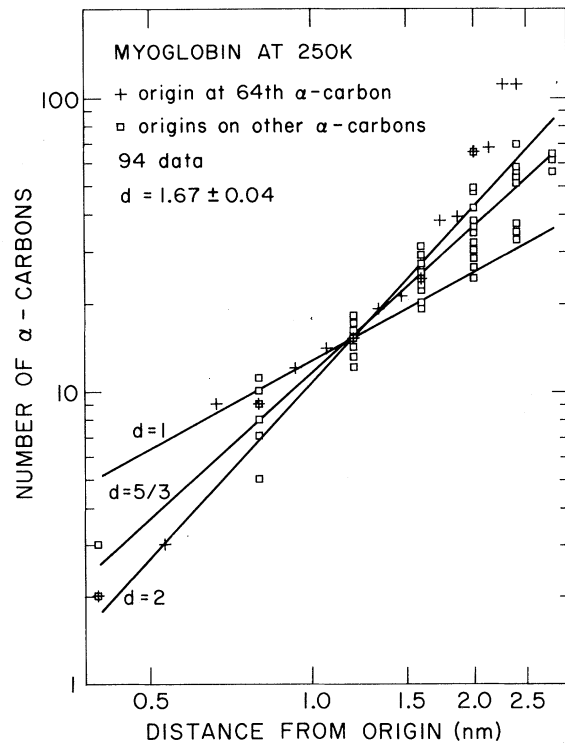


FIG. 2. The number of alpha carbons ( $2 \leq N \leq 85$ ) within a sphere of radius  $R$ , subject to the condition that there exists a path along the backbone from each alpha carbon to the origin which does not leave the sphere. The circles are the data for several origins situated on each of 17 alpha carbons in contact with the heme plane as well as the alpha carbon nearest the center of mass of the backbone. Many of the circles are multiple points. The crosses are the data for one of the alpha carbons in contact with the  $\text{Fe}^{3+}$  ion (No. 64), with use of a smaller step in  $R$ . Shown are lines for dimensions of 1, 2, and (the least-squares fit of) 1.67.

caption. This figure makes clear that the number varies approximately as the  $\frac{5}{3}$  power of distance.<sup>16</sup> The data with the 64th alpha carbon as the origin, show a staircase effect, and is found with all other origins. The data are clearly inconsistent with fractal dimensions of 1 or 2. This confirms that the protein is a fractal of approximate dimension  $\frac{5}{3}$ , thus giving strong independent support to the analysis of protein vibrations and spin relaxation presented here.

We note finally that flexing modes probably dominate the low-frequency spectrum at low temperatures when bond conformational changes are frozen out. The quantity  $\epsilon$  simultaneously measures the bond strain and the correlation factor<sup>17</sup> of the SAW for this case. The temperature range

1–20 K is associated with wavelengths of  $\approx 10$ – $10^3$  bonds. Environmental constraints on the backbone presumably have only minor effects on these long-wavelength vibrations, or act alternatively as additional pinning points of the type that occur normally in a SAW.

This work was supported in part by the U. S. Public Health Service under Grant No. GM-24488 and by the U. S. Department of Energy under Contract No. DE-AC02-76ER01198. We wish also to acknowledge the assistance of Hans Frauenfelder in providing us with the myoglobin x-ray data, Gerald Wagner for biochemical advice, and Trevor Colvin for assistance in the experiments.

<sup>1</sup>R. C. Herrick and H. J. Stapleton, *J. Chem. Phys.* **65**, 4778 (1976).

<sup>2</sup>Colin Mailer and C. P. S. Taylor, *Biochim. Biophys. Acta* **322**, 195 (1973).

<sup>3</sup>R. Orbach and H. J. Stapleton, in *Electron Paramagnetic Resonance*, edited by S. Geschwind (Plenum, New York, 1972), Chap. 2.

<sup>4</sup>B. B. Mandelbrot, *Fractals* (Freeman, San Francisco, 1977).

<sup>5</sup>K. W. H. Stevens, *Rep. Prog. Phys.* **30**, 189 (1967).

<sup>6</sup>J. C. Gill, *Rep. Prog. Phys.* **38**, 91 (1975).

<sup>7</sup>T. Bray, G. C. Brown, Jr., and A. Kiel, *Phys. Rev.*

**127**, 730 (1962).

<sup>8</sup>A. Rannestad and P. E. Wagner, *Phys. Rev.* **131**, 1953 (1963).

<sup>9</sup>We have fit all the relaxation data of Ref. 2 (except the 18.5-K datum) to a function of the form  $A + BT^n$ , with  $A = (2.23 \pm 0.38) \times 10^5 \text{ s}^{-1}$ ,  $B = 0.12 \pm 0.17 \text{ s}^{-1}$ , and  $n = 6.55 \pm 0.52$ . The straight line in Fig. 4 of Ref. 2 fits a power law, with  $n$  approximately equal to 6.0.

<sup>10</sup>The MbN<sub>3</sub> and CP450 data of Fig. 1 are also well fitted by Eq. (2) with  $p = 2$  and  $\Theta$  values of 54.3 and 57.0 K, respectively.

<sup>11</sup>Haywood Blum and Tomoko Ohnishi, *Biochim. Biophys. Acta* **621**, 9 (1980).

<sup>12</sup>Jean-Pierre Gayda, Patrick Bertrand, Alain Deville, Claude More, Guy Roger, John F. Gibson, and R. Cammack, *Biochim. Biophys. Acta* **581**, 15 (1979).

<sup>13</sup>See P. J. Flory, *Principles of Polymer Chemistry* (Cornell Univ. Press, Ithaca, N.Y., 1953).

<sup>14</sup>J. C. Le Guillou and J. Zinn-Justin, *Phys. Rev. Lett.* **39**, 95 (1977); Ronnie Barr, Chava Brender, and Melvin Lax, *J. Chem. Phys.* **72**, 2702 (1980).

<sup>15</sup>Hans Frauenfelder, Gregory A. Petsko, and Demetrius Tsenoglu, *Nature (London)* **280**, 558 (1979).

<sup>16</sup>The dimensionality  $d$  we calculate in Fig. 2 is related to the root-mean-square end-to-end length ( $R_N^{\text{rms}}$ ) of a polymer containing  $N$  monomers by  $R_N^{\text{rms}} \propto N^{1/d}$ . See for example, Ralph Grishman, *J. Chem. Phys.* **58**, 220 (1973).

<sup>17</sup>See C. P. Flynn, *Point Defects and Diffusion* (Oxford Univ. Press, London, 1972).